[Frontiers in Bioscience 9, 1082-1099, May 1, 2004]

# MACROSCOPIC ELECTROSTATIC MODELS FOR PROTONATION STATES IN PROTEINS

**Donald Bashford**

*Department of Molecular Biotechnology, Hartwell Center, Saint Jude Children's Research Hospital, Memphis, TN, USA*

## TABLE OF CONTENTS



## 1. ABSTRACT

The use of macroscopic electrostatic models to calculate the relative energetics of protonation states and the pH-titration properties of ionizable groups in proteins is described. These methods treat the protein as an irregularly-shaped low-dielectric object containing embedded atomic charges immersed in a high-dielectric (solvent) medium. The energetics of altering protonation states then involves the electrostatic work of altering the embedded atomic charges. The governing electrostatic equation is either the Poisson or linearized Poisson–Boltzmann equation, which generally requires numerical solution. A tutorial approach is taken, the main aim of which is a thorough understanding of the method.

## 2. INTRODUCTION

The prediction of the pH-titration properties of ionizable sidechains in proteins using macroscopic electrostatic models has been important for the development and validation of models of protein electrostatics. As these calculations have enjoyed more success, they have also become a useful tool for a quantitative understanding of protein function, particularly where internal proton transfers or the maintenance of unusual protonation states is important for protein function. The focus of this article is the use of models that combine macroscopic electrostatics with the details of the atomic structure of proteins. We refer to this class of models by the acronym MEAD, for macroscopic electrostatics with atomic detail. The quintessential MEAD model (1) depicts the protein as a region of low dielectric constant with partial atomic charges at the positions of the nuclei, surrounded by a high dielectric medium, the solvent. The boundary between the interior, low-dielectric region and the exterior, high-dielectric regions is a surface defined by the atomic coordinates and radii of the protein. Typically, Connolly's definition of the molecular surface (2) is used, though other definitions (3) are also possible.

Although many papers and several reviews have appeared reporting the use of such a model to predict pH-titration properties and the relative energetics of protonation states in proteins (4,5), they have usually only described the methods briefly. The significant formal and practical difficulties that arise in formulating these methods in detail have either not been discussed, or are mentioned only in passing. It has been the author's experience that this lack of a deeper description of the method is often an obstacle for researchers new to the methods who wish to do such calculations for themselves. It is therefore the aim of this article to bring these details out from the in-house lore of a few research groups, or the internals of specialized software, so that the methods can be more accessible, and their pitfalls and possibilities better understood by a wider audience.

We begin with a brief introduction to the macroscopic Poisson equation for non-uniform dielectric

environments, the linearized Poisson–Boltzmann (LPB) theory for electrolytes, and the use of Green functions as a way of exploiting the linearity of these equations. The calculation of electrostatic energy is discussed in some detail, with particular attention paid to the problem of point-like charges embedded in a macroscopic media, and need to cancel out spurious infinite terms in calculations of energy differences. The finite-difference method of solving the Poisson or LPB equation is discussed next, not so much to detail the method itself as to point out some issues particular to the use of this or other numerical methods to implement MEAD models. Before describing the application of these ideas to protonation states in proteins, we describe their application to the closely related problem of small-molecule solvation and $pK_a$.

Nearly all of the methods described here are implemented in the author's computer program suite, MEAD. (Typewriter typeface distinguishes the program suite, MEAD, from the model, MEAD). MEAD is available in source-code form through the author's web site, http://www.scripps.edu/bashford, or by anonymous FTP from ftp.scripps.edu, in the directory pub/electrostatics. Modification and redistribution of MEAD is allowed under the terms of the GNU General Public License (6). Soon, MEAD will be available from a new web site to be established at the institution to which the author has recently moved, Saint Jude Children's Research Hospital. Contact Don.Bashford@stjude.org for details.

## 3. MACROSCOPIC ELECTROSTATICS

In vacuum electrostatic theory, the electric field $\mathbf{E}$ is determined by Gauss's law, which, in its differential form, states that the divergence of the electric field is proportional to the charge density; specifically,

$$\nabla \cdot \mathbf{E} = 4\pi\rho. \qquad (1)$$

(In these expressions, and elsewhere in this article, we use the Gaussian system of units, in which a factor of $4\pi$ appears in the Gauss law, but not in the Coulomb law (7).) The further condition that $\mathbf{E}$ is curl-free implies that it is the gradient of a scalar potential. It is conventional to define the electrostatic potential by $\mathbf{E} = -\nabla\phi$. Substitution leads to the vacuum Poisson equation,

$$\nabla^2\phi = -4\pi\rho. \qquad (2)$$

The macroscopic version of the Gauss law is

$$\nabla \cdot \mathbf{D} = 4\pi\rho, \qquad (3)$$

where $\mathbf{D}$ is the electric displacement, defined by $\mathbf{D} = \varepsilon\mathbf{E}$, where $\varepsilon$ is the dielectric constant. Substitution to obtain $\mathbf{D}$ in terms of $\phi$ leads to,

$$\nabla \cdot \left[\varepsilon(\mathbf{r})\nabla\phi(\mathbf{r})\right] = -4\pi\rho(\mathbf{r}), \qquad (4)$$

which is the macroscopic version of the Poisson equation. The simple proportionality of $\mathbf{D}$ to $\mathbf{E}$ involves the assumption that the polarization of the medium is proportional to the electric field. That is, linear response is assumed.

### 3.1. Outer Boundary Conditions

Eqs. 2 or 4 are not enough to define the potential uniquely. For example if $\phi$ satisfies Eq. 2, then one can add to it any function $\phi'$ for which $\nabla^2\phi' = 0$, and the resulting function will still satisfy the Poisson equation. In order to define a unique solution within some region, one must also specify *boundary conditions*, relations that $\phi$ must satisfy at the boundary of the region. The most common kind are Dirichlet boundary conditions, in which the value of the potential on the boundary is specified. Examples are,

$$\phi(\mathbf{s}) = 0 \qquad (5)$$

$$\phi(\mathbf{s}) = f(\mathbf{s}), \qquad (6)$$

where $f$ is a function defined on all surface points, $\mathbf{s}$. The first expression, in which the potential is required to be zero on the boundary is called a *homogeneous* Dirichlet boundary condition. The second is a general Dirichlet condition. It can be shown that for any charge distribution and any Dirichlet boundary condition, there exists one and only one solution to the Poisson equation.

Another type of boundary condition is the von Neumann type, in which the derivative of the potential in the direction perpendicular to the boundary is specified all around the boundary. Again there are both homogenous (the derivative is zero) and more general variants. The von Neumann conditions only define the potential to within an additive constant, since adding a constant to $\phi$ does not change its derivative. However, the physical significance of $\phi$ comes only from its derivatives (which determine the electric field force) or from differences of $\phi$ at different points (which determine the work of moving a charge from point to point), so adding a constant to $\phi$ has no physical significance.

The boundary condition we shall generally be concerned with here is that $\phi$ must go to zero as points become infinitely far from the charge distribution under consideration. This is a boundary condition of the homogenous Dirichlet type.

### 3.2. Linear Response and Green Functions

For a potential determined by the Poisson equation and a homogenous Dirichlet boundary condition, the manner in which a charge distribution produces an electric field or potential is *linear*. This means that increasing the charge by some factor increases the field by that same factor. It is also *additive* in that the field or potential produced by the sum of two charge distributions is equal to the sum of the potentials or fields that would be produced by the individual charge distributions. Mathematically, these properties arise from the fact that the equations for the potential, Eqs. 2 or 4, are *linear* and *homogenous* in $\phi$ and $\rho$. Linearity in $\phi$ (or $\rho$) means that in all terms in which $\phi$ (or $\rho$) appears, only linear operations are applied to it. A linear operation is one that

has the property that if it is applied to a linear combination of operands, the result is an equivalent linear combination of the results of applying the operator to the individual operands. That is, if $f$ and $g$ are functions to which a linear operator $L$ can be applied, and $a$ and $b$ are constants, then

$$L(af + bg) = a(Lf) + b(Lg). \qquad (7)$$

Differentiation of a function, or multiplication by a constant are examples of linear operators. One can easily verify that the operations on $\phi$, $\nabla^2$ in Eq. 2 or $\nabla \cdot \varepsilon \nabla$ in Eq. 4, are linear; and the multiplication of $\rho$ by $-4\pi$ in both equations is also linear. Homogeneity in $\phi$ and $\rho$ means that every term is either linear in $\phi$ or linear in $\rho$ (but not both: there are no $\rho\phi$ terms). By exploiting these properties, it easily can be shown that if,

$$\nabla \cdot \left[\varepsilon \nabla \phi_1\right] = -4\pi\rho_1 \qquad (8)$$

$$\nabla \cdot \left[\varepsilon \nabla \phi_2\right] = -4\pi\rho_2 \qquad (9)$$

then

$$\nabla \cdot \left[\varepsilon \nabla (a\phi_1 + b\phi_2)\right] = -4\pi(a\rho_1 + b\rho_2). \qquad (10)$$

This is the mathematical statement of the linear and additive character of the potential's dependence on the charge.

The linearity of the vacuum Poisson equation (2) arises from fundamental physics. However, the linearity of the macroscopic Poisson equation (4) arises because the polarization of the medium is assumed to be a linear function of the electric field. This is an example of *linear response*, and is generally only valid if the fields are sufficiently small.

Systematic explorations of the ways in which linearity and additivity can be exploited can be carried out using *Green functions*. The Green function associated with a particular Poisson equation and homogenous Dirichlet boundary condition is the function whose value $g(\mathbf{r},\mathbf{r}')$ is equal to the potential that would be produced at point $\mathbf{r}$ if a unit point charge were placed at the position $\mathbf{r}'$, assuming the potential is governed by that particular Poisson equation and boundary condition [1]. For example, the green function for the vacuum Poisson equation and the boundary condition, $\phi(\mathbf{r}) \to 0$ as $\mathbf{r} \to \infty$, is the familiar Coulomb formula for a potential due to a unit charge:

$$g(\mathbf{r},\mathbf{r}') = \frac{1}{|\mathbf{r} - \mathbf{r}'|}. \qquad (11)$$

For the macroscopic Poisson equation (4) the Green function depends on the details of the dielectric properties of the space, as expressed through the function $\varepsilon(\mathbf{r})$.

For a distribution of point charges: $q_1$ at position, $\mathbf{r}_1$, $q_2$ at $\mathbf{r}_2$, etc., the properties of linearity and additivity mean that the total potential can be expressed in terms of the Green function as,

$$\phi(\mathbf{r}) = \sum_i^N q_i g(\mathbf{r},\mathbf{r}_i). \qquad (12)$$

For a continuous charge distribution $\rho$ an analogous formula applies:

$$\phi(\mathbf{r}) = \int_V \rho(\mathbf{r}') g(\mathbf{r},\mathbf{r}')\, d\mathbf{r}', \qquad (13)$$

where $V$ is a volume that contains the charge distribution. The Green function depends only on the dielectric properties of the space and the boundary conditions around that space, and not on the charges. The potential arising from any charge distribution can be obtained by summation or integration using the Green function.

## 4. ELECTROLYTES AND THE LINEARIZED POISSON–BOLTZMANN (LPB) EQUATION

Let $\rho$ denote the fixed charge distribution, and $\phi$ the potential arising from *both* the fixed and mobile charges. Let $n_A(\mathbf{r}), n_B(\mathbf{r}), \ldots$ represent the local number density of mobile ion species, A, B, ..., having valence $Z_A, Z_B, \ldots$. Overall electro-neutrality of the solution requires that

$$Z_A c_A + Z_B c_B + \cdots = 0, \qquad (14)$$

where the $c$ are the average concentrations of the species, expressed as numbers of particles per unit volume. In regions where $\phi$ is negative, the local concentration of positive ions should increase, while the concentration of negative ions should decrease; and vice versa in regions of positive $\phi$. These local changes should follow Boltzmann statistics, so we expect $n_A(\mathbf{r}) \propto \exp(-eZ_A\phi(\mathbf{r})/kT)$, where $e$ is the proton charge, and $k$ is the Boltzmann constant. In regions far from the fixed charge, $\phi$ should become zero because of the overall electro-neutrality of the solution and $n_A$ is expected to revert to its average value $c_A$. The relation of $n_A$ to $\phi$ that satisfies these requirements is $n_A(\mathbf{r}) = c_A \exp(-eZ_A\phi(\mathbf{r})/kT)$. This means that the overall charge density, including both the fixed and mobile densities, is

$$\rho_{\text{tot}}(\mathbf{r}) = \rho(\mathbf{r}) + \Theta_{\text{iacc}}(\mathbf{r})\left[eZ_A c_A \exp(-eZ_A\phi(\mathbf{r})/kT) + eZ_B c_B \exp(-eZ_B\phi(\mathbf{r})/kT) + \cdots\right], \qquad (15)$$

where $\Theta_{\text{iacc}}$ is a step function whose value is 1 in ion-accessible regions, and 0 in ion-inaccessible regions, such as the interior of a macromolecule. To obtain an equation for $\phi$ that accounts for its dependence on both fixed and mobile charges, $\rho_{\text{tot}}$ is substituted for the $\rho$ in the macroscopic Poisson equation, 4:

$$\nabla \cdot \varepsilon \nabla \phi + 4\pi e \Theta_{\text{iacc}}\left[Z_A c_A \exp(-eZ_A\phi/kT) + Z_B c_B \exp(-eZ_B\phi/kT) + \cdots\right] = -4\pi\rho \qquad (16)$$

This is the Poisson–Boltzmann equation (8).

Unlike the Poisson equation, the Poisson–Boltzmann equation is non-linear because of the appearance of $\phi$ in the exponential terms. This means that the linear superposition properties discussed in Sec. 3.2 do not apply, nor do the energy expressions to be developed in Sec. 5. The Poisson–Boltzmann equation is only an approximation to the effect of mobile ions, because in its derivation, the effect of hard-sphere repulsion between ions and the effect of ion–ion correlations have been neglected.

The Poisson–Boltzmann equation, 16, can be linearized by expanding the exponentials in powers of $\phi$ :

$$\exp(-eZ_A\phi/kT) = 1 - eZ_A\phi/kT + \frac{1}{2}(eZ_A\phi/kT)^2 - \cdots \quad (17)$$

If terms of order $(eZ_A\phi/kT)^2$ and higher are neglected, the Poisson–Boltzmann equation becomes,

$$\nabla\cdot\varepsilon\nabla\phi + 4\pi e\Theta_{\text{iacc}}\left[Z_Ac_A + Z_Bc_B + \cdots - Z_A^2c_Ae\phi/kT - Z_B^2c_Be\phi/kT - \cdots\right] = -4\pi\rho \quad (18)$$

Because of the electro-neutrality condition (Eq. 14) the zero-order terms, such as $Z_Ac_A$ , sum to zero. The result can be written as

$$\nabla\cdot\varepsilon(\mathbf{r})\nabla\phi(\mathbf{r}) - \kappa^2(\mathbf{r})\varepsilon(\mathbf{r})\phi(\mathbf{r}) = -4\pi\rho(\mathbf{r}) \quad (19)$$

where

$$\kappa^2(\mathbf{r}) = \Theta_{\text{iacc}}(\mathbf{r})\frac{8\pi e^2 I}{\varepsilon(\mathbf{r})kT} \quad (20)$$

$$I = \frac{1}{2}[Z_A^2c_A + Z_B^2c_B + \cdots] \quad (21)$$

The last expression is the standard definition of the ionic strength in units of ion numbers per volume. Equation 19 is the Linearized Poisson Boltzmann equation (LPB).

We now have an equation for the potential that includes electrolyte effects (albeit approximately) and is linear. Therefore, the linear and additive properties discussed in Sec. 3.2 can be exploited and analyzed in terms of Green functions.

The theory outlined here is often referred to as Debye–Hückel theory (9). Its more familiar formulae, which provide a meaning for $\kappa$ , are obtained in the special case where the dielectric constant has the same value $\varepsilon$ throughout all space and the mobile ions are free to move everywhere. Eq. 19 then becomes,

$$\nabla^2\phi - \kappa^2\phi = -\frac{4\pi\rho}{\varepsilon} \quad (22)$$

and its Green function is,

$$g(\mathbf{r},\mathbf{r}') = \frac{\exp(-\kappa|\mathbf{r}-\mathbf{r}'|)}{\varepsilon|\mathbf{r}-\mathbf{r}'|}. \quad (23)$$

In contrast to the long-ranged Coulombic potential, the potential in an electrolyte dies off exponentially with a characteristic length $\kappa^{-1}$ , which is inversely proportional to the square root of the ionic strength. Eq. 23 is often called the Debye formula, and $\kappa^{-1}$ is called the Debye length.

## 5. ELECTROSTATIC ENERGY AND MOLECULES

Most applications of the MEAD model to molecular properties, including the prediction of p$K_a$ values and protonation states, involve calculation of the electrostatic work required to assemble some particular charge distribution within some specified dielectric and electrolyte environment. Since the charge distribution typically includes point charges, the resulting electrostatic potential will include *Coulomb singularities:* points where the potential rises to infinity as one approaches the point charge like the limit of $1/r$ as $r$ goes to zero. When analytical solutions for the potential are available, these singularities can simply be omitted based on the argument that they merely represent the (infinite) work needed to squeeze a finite amount of charge onto an infinitesimal point—a process in which we are not interested. However, in typical applications the potential must be solved for by numerical methods such as finite differences, which do not give the potential separated into singular and non-singular parts. Rather, the singularities are mixed into the result as finite (but large) contributions to the potential whose value is an artifact of the numerical method. This means that in developing methods, one must keep track of singularities and arrange a suitable subtraction that removes them. The Green function formalism introduced in Sec. 3.2 is well suited to this purpose.

In applications to molecules one is often interested in the free energy associated either with moving a molecular charge distribution from one environment to another (as in the case of solvation of polar molecules), or with alteration of the charge distribution within some fixed environment (as in the case of electron transfer or proton transfer). For either case, a useful starting point is the electrostatic work of creating a charge distribution in an environment of fixed dielectric and electrolyte properties (represented by $\varepsilon(\mathbf{r})$ and $\kappa^2(\mathbf{r})$ ) that is initially empty of charge and in which the initial electrostatic potential is zero. This quantity corresponds to a free energy if we regard the charge distribution being built up as a mechanical extensive variable (10).

The incremental work of adding an increment of charge $\delta\rho$ is

$$\delta W = \int_V \phi(\mathbf{r})\delta\rho(\mathbf{r})\,d^3\mathbf{r} \quad (24)$$

where $\phi$ is the potential due to the charge already present. Assuming that the governing electrostatic equations are linear (e. g., the Poisson or LPB equations), the dependence of $\phi$ on the density already present can be expressed in terms of the Green function for the dielectric and boundary environment, leading to

$$\delta W = \int_V\int_V \rho(\mathbf{r}')g(\mathbf{r},\mathbf{r}')\,d^3\mathbf{r}'\delta\rho(\mathbf{r})\,d^3\mathbf{r}. \quad (25)$$

The total work $W$ of creating the charge distribution $\rho$ is found by integrating this expression over the $\delta\rho$ , from a zero charge distribution to the full charge distribution. This gives,

$$W = \frac{1}{2}\int_V \int_V \rho(\mathbf{r})\rho(\mathbf{r}')g(\mathbf{r},\mathbf{r}')\,d^3\mathbf{r}'\,d^3\mathbf{r}, \quad (26)$$

which can be understood as the electrostatic interaction of the charge distribution $\rho$ with itself, via the interaction kernel provided by the Green function $g$. Using equation 13, this can be written,

$$W = \frac{1}{2}\int_V \rho(\mathbf{r})\phi(\mathbf{r})\,d^3\mathbf{r}, \quad (27)$$

which means that the work required to create the distribution $\rho$ can be found by first solving the Poisson equation for the potential due to the distribution, and then applying the above formula [2].

In typical applications to molecules, $\rho$ is a molecular charge distribution that is confined to a molecular interior that has some uniform dielectric constant $\varepsilon_{\text{in}}$, and is not accessible to the mobile ions of the electrolyte (i.e., $\kappa^2(\mathbf{r}) = 0$ in the interior). In this case it can be shown that the Green function always has the form:

$$g(\mathbf{r},\mathbf{r}') = \frac{1}{\varepsilon_{\text{in}}|\mathbf{r}-\mathbf{r}'|} + g_r(\mathbf{r},\mathbf{r}'), \quad (28)$$

where it is understood that both $\mathbf{r}$ and $\mathbf{r}'$ are confined to the interior. The first term is the Coulombic green function and has a $1/r$ singularity; and the second term is the *reaction potential* term and is smoothly varying and free of singularities in the interior region. The reaction potential arises due to the presence of dielectrics different from $\varepsilon_{\text{in}}$ in the exterior region and from the electrolyte. In the case where $\varepsilon_{\text{in}} = 1$ (a non-polarizable interior) the reaction term is the potential at $\mathbf{r}$ due the polarization and mobile ion rearrangement in the external environment that is produced in reaction to a unit charge at $\mathbf{r}'$. For $\varepsilon_{\text{in}} > 1$ it is related to the difference between the exterior polarization and the polarization that an exterior medium of dielectric $\varepsilon_{\text{in}}$ would have. The electrostatic work expression becomes

$$W = \frac{1}{2}\int_{\text{in}} \frac{\rho(\mathbf{r})\rho(\mathbf{r}')}{\varepsilon_{\text{in}}|\mathbf{r}-\mathbf{r}'|}d^3\mathbf{r}\,d^3\mathbf{r}' + \frac{1}{2}\int_{\text{in}} \rho(\mathbf{r})\rho(\mathbf{r}')g_r(\mathbf{r},\mathbf{r}')\,d^3\mathbf{r}\,d^3\mathbf{r}', \quad (29)$$

where the integration volume is confined to the interior region.

Typically, the molecular charge distribution is given as a set of point charges (such as atomic partial charges) located at the positions of the atomic nuclei. To pass from the continuous $\rho$ form of the charge distribution to a point-like form, consider a distribution in which for each atom $i$, there is an atomic charge $q_i$ distributed uniformly in a small sphere of radius $R_i$ about the atomic nucleus located at $\mathbf{r}_i$. If the sphere radii are very small compared to interatomic distances, then to a very good approximation the work expression can be integrated to obtain a simple summation over charges and charge pairs:

$$W \approx \sum_i \frac{q_i^2}{2\varepsilon_{\text{in}}R_i} + \frac{1}{2}\sum_{ij,j\neq i}\frac{q_iq_j}{\varepsilon_{\text{in}}|\mathbf{r}_i-\mathbf{r}_j|} + \frac{1}{2}\sum_{ij} q_iq_jg_r(\mathbf{r}_i,\mathbf{r}_j) \quad (30)$$

$$= \sum_i \frac{q_i^2}{2\varepsilon_{\text{in}}R_i} + \sum_{ij,j>i}\frac{q_iq_j}{\varepsilon_{\text{in}}|\mathbf{r}_i-\mathbf{r}_j|} + \frac{1}{2}\sum_i q_i\phi_r(\mathbf{r}_i) \quad (31)$$

The first term in Eq. 30 is the Coulombic interaction of each sphere with itself; the second term is the Coulombic interaction between spheres; and the third is the interaction of the spheres with themselves and each other through the reaction potential. In Eq. 31, the reaction term is written in terms of the reaction potential using the relation $\varphi_r(\mathbf{r}) = \sum_j q_j g_r(\mathbf{r},\mathbf{r}_j)$ (see Eq. 12).

As the spheres containing the atomic charge are made infinitesimally small ($R_i \to 0$), the approximations used in Eq. 30 become exact, but the first term, the Coulomb self-energy term, becomes infinite. As mentioned above, such infinite terms are generally not of interest, so one approach is to simply leave them out. But this can only be done if the reaction potential $\phi_r$ is available in some practical form. Here we take a more formal approach based on the observation that one is usually interested in calculating free energy differences, rather than the absolute free energy of some particular electrostatic arrangements, and in many cases the problematic Coulomb self-energy terms cancel out. For example, calculation of solvation energies (see Sec. 7) involves a difference of $W$ for two different *exterior* dielectric environments, while $\varepsilon_{\text{in}}$ and the charges and their positions remain the same. In that case all but the reaction-potential terms cancel out. For the electrostatic energy of a conformational change, the charges and $\varepsilon_{\text{in}}$ again remain the same, but their positions change and the shape of the boundary between interior and exterior may change. In this case, both the reaction term and the interatomic Coulomb terms change and contribute to the difference. In general, the Coulombic self-energy terms will cancel for the electrostatic free energy difference associated with any process obeying the following restrictions:

1. The internal dielectric constant $\varepsilon_{\text{in}}$ does not change.

2. No charge is moved from the interior region to a region with a different dielectric constant.

3. The the charges $q_i$ are not altered.

For most processes of interest the first two conditions are easily met. The third appears more problematic, since protonation and deprotonation involve changes of the atomic partial charge, but we shall see in that this can be handled by reference to a model process in which the relevant energies are presumed to by known or calculable by other means.

## 6. THE FINITE-DIFFERENCE METHOD

The Poisson equation (Eq. 4) or the LPB equation (Eq. 19) are examples of elliptic partial differential equations, the numerical solution of which is a large branch of applied mathematics whose review is beyond the scope

of this article. We shall only deal with one particular method that is commonly used to implement MEAD models, the finite-difference method. It is relatively simple, and quite flexible in terms of the dielectric and electrolyte environments that can be handled, and it is competitive with alternative methods in terms of computational cost for many applications to biological molecules. Some accuracy issues have been explored for the specific application of the method to biomolecules (11,12,13). Rather than describe the method fully or generally, we give the basic ideas, some details of how they are applied to the Poisson or LPB equations arising in MEAD models, and some discussion of how the problem of infinite Coulomb self energies plays out on the finite-difference grid.

The essential idea is to approximate derivatives as differences between function values sampled at points a finite distance apart. Consider only the $x$ component of the double gradient, $\nabla \cdot [\varepsilon \nabla \phi]$ occurring in Eqs. 4 and 19, and let $h$ be the distance between sampling points:

$$\begin{aligned}\frac{\partial}{\partial x}\left[\varepsilon(\mathbf{r})\frac{\partial}{\partial x}\phi(\mathbf{r})\right] &\approx \frac{1}{h}\left[\varepsilon(x+\frac{h}{2},y,z)\frac{\partial\phi(\mathbf{r})}{\partial x}\bigg|_{\mathbf{r}=(x+\frac{h}{2},y,z)} - \varepsilon(x-\frac{h}{2},y,z)\frac{\partial\phi(\mathbf{r})}{\partial x}\bigg|_{\mathbf{r}=(x-\frac{h}{2},y,z)}\right] \\ &\approx \frac{1}{(h)^2}\left[\varepsilon(x+\frac{h}{2},y,z)\big(\phi(x+h,y,z)-\phi(x,y,z)\big) - \varepsilon(x-\frac{h}{2},y,z)\big(\phi(x,y,z)-\phi(x-h,y,z)\big)\right]\end{aligned}$$

Note that samples of $\phi$ and $\varepsilon$ are both taken at intervals of $h$ but the $\varepsilon$ points are shifted by $h/2$ relative to the $\phi$ points. Extending this idea to three dimensions and replacing functions defined in three-dimensional space by values defined on a three-dimensional cubic lattice with spacing $h$, and lattice indices $ijk$, the LPB equation (Eq. 19) becomes:

$$\frac{1}{h^2}\Big[\phi_{i+1\,jk}\varepsilon_{i+\frac{1}{2}\,jk} + \phi_{i-1\,jk}\varepsilon_{i-\frac{1}{2}\,jk} + \phi_{i\,j+1\,k}\varepsilon_{i\,j+\frac{1}{2}\,k} + \phi_{i\,j-1\,k}\varepsilon_{i\,j-\frac{1}{2}\,k} \qquad (32)$$

$$+\phi_{ij\,k+1}\varepsilon_{ij\,k+\frac{1}{2}} + \phi_{ij\,k-1}\varepsilon_{ij\,k-\frac{1}{2}} - 6\phi_{ijk}\bar{\varepsilon}_{ijk}\Big] - \kappa^2_{ijk}\bar{\varepsilon}_{ijk}\phi_{ijk} = 4\pi q_{ijk}/h^3$$

where $\bar{\varepsilon}_{ijk}$ is defined as the value of $\varepsilon$ averaged over the six surrounding half-integer grid points, and $q_{ijk}$ is the charge assigned to the grid point. Requiring this equation to be satisfied for all $ijk$ (except the outer face points of the grid) results in a large system of linear equations for the values on the $\phi$ lattice. The values of $\phi$ on the outer face points must be supplied as input. This corresponds to the Dirichlet boundary conditions required to supplement the Poisson or LPB equations. Perhaps the most straightforward practical technique for solving this type of system is the successive over-relaxation (SOR) method, but conjugate gradient and multigrid methods are also commonly used. Descriptions of these methods for the non-specialist can be found in references (14) and (15), and more detailed treatments can be found in (16).

Several points particular to the set-up of finite difference problems for MEAD models deserve comment. First, one usually is interested in the Dirichlet boundary condition $\phi \to 0$ at infinity, but the finite size of the grid forces one to define $\phi$ on the the faces of grid. For the Poisson–Boltzmann equation, setting $\phi$ to zero on the boundary can be a satisfactory simulation of the desired infinite boundary condition provided there is an electrolyte-filled region spanning several Debye lengths between the molecule under study and the outer faces, since the potential falls exponentially to zero at such distances (see Eq. 23). Setting the boundary potential to zero in the absence of electrolyte may be a poor choice, particularly for charged molecules, because the true potential falls off only as $1/r$. A reasonable approximation in this case is a Coulomb formula with the dielectric constant set to that of the exterior region (e. g., the solvent) provided there is a sufficiently long span of exterior region between the faces and any part of the molecule under study. At worst, the boundary potential will be off by a dipole term that falls off like $1/r^2$, and the worst errors in the potential will occur far outside the molecule, whereas one is generally only interested in the potential inside the molecule. In the author's experience, a 15 Å span provides reasonable accuracy.

These considerations often require the grid to span a large volume, but since the cost of the calculations rises rapidly with the number of grid points, this comes into conflict with the goal of obtaining good accuracy in the underlying finite-difference approximation for which one would like to have a grid spacing $h$ that is small compared to typical interatomic distances. (In the author's experience $h = 0.25$ Å gives reasonable accuracy.) For a cubic grid having $L$ points along each edge, the memory required to store the values on the grid obviously rises like $L^3$. The processor time required for the solution of the finite difference problem by the SOR method rises at a rate between $L^4$ and $L^5$, Multigrid methods (15) provide much better scaling of processor requirements at the expense of more complex code and a modest increase in memory requirements, and set-up overhead. A common way around the grid-extent versus grid-spacing trade-off is to exploit the fact that one is typically only interested in finding the potential accurately in the interior region of the molecule or some "interesting" part of a molecule (such as a titratable protein sidechain). One can therefore make an initial calculation with an grid of large extent and coarse spacing, followed by calculations on finer grids of smaller extent lying within the coarse grid's extent and centered on the interesting region. The boundary conditions for the fine-grid calculations are obtained by interpolation from the course grid. This technique is often called focusing (11), and there can be multiple levels of focusing (i.e., finer grids within the fine grids, etc.).

Another point particular to MEAD models concerns the $\varepsilon$ grid. It would appear to require three times as much storage as the $\phi$ grid since $\varepsilon$ must be defined at the halfway points along the $x$, $y$ and $z$ direction between $\phi$ grid points. However, MEAD models typically have large regions of uniform dielectric constant separated by sharp transitions (e. g., the boundary between the

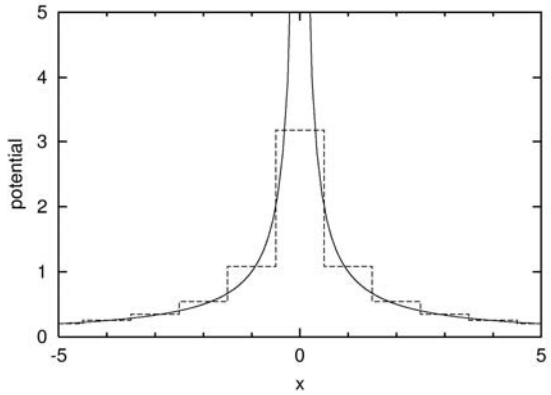


**Figure 1.** The Coulomb singularity and and its finite-difference counterpart. The result of a finite difference calculation for the potential in vacuum due to a unit charge on the origin using a grid spacing, $h = 1.0$ is shown histogram style, together with the analytical solution $1/x$. The finite difference solution has a finite value, $\approx 3.18q/h$, at the location of the charge.

molecular interior and exterior region), with the result that the vast majority of the grid points are in regions where the dielectric is uniform between the grid point and its nearest neighbor. For such points, the values of $\varepsilon_{i+\frac{1}{2}jk}$, etc. are all identical to $\varepsilon_{ijk}$ and Eq. 32 can be simplified to

$$\frac{1}{h^2}\left[\phi_{i+1jk}+\phi_{i-1jk}+\phi_{ij+1k}+\phi_{ij-1k}+\phi_{ijk+1}+\phi_{ijk-1}-6\phi_{ijk}\right]-\kappa^2_{ijk}\phi_{ijk}=4\pi q_{ijk}/(h^3\varepsilon_{ijk}) \quad (33)$$

This means that $\varepsilon$ grid values actually only need be stored for grid points near the dielectric boundaries. Large savings in processor time are also obtainable since the iterative methods need only evaluate an expression similar to Eq. 33 rather than Eq. 32 at most grid points. Exploitation of this can give a speedup factor of order 10. Most general purpose elliptic finite-difference solvers do not exploit this rather special property of the Poisson problems arising from MEAD models, whereas the packages specialized to molecular electrostatics (such as `MEAD`(17,18) and `DelPhi` (19)) do exploit it and give much better performance.

The Coulomb self-energy problem comes up in a new guise in the finite difference method. The result of making a finite difference calculation for the potential due to a single charge on a central grid point and a uniform dielectric constant is sketched in Figure 1 along with a plot of the $1/r$ analytical form of the Coulomb potential. Rather than rising to infinity as the center is approached, the finite difference solution takes on a finite value at the central point, and this value is dependent on the grid spacing — specifically, it is inversely proportional to the spacing. This means that if one attempts to use an expression analogous to Eq. 27 using a potential calculated by the finite difference method and a point charge distribution, the result will contain large spurious "grid singularity" contributions as well as the physically meaningful charge–charge interactions and reaction field contributions. These spurious contributions can be subtracted out in energy difference calculations of the kind described at the end of Sec. 5, but in addition to the restrictions listed there, the two calculations must use grids with the same spacing and the charges must be mapped onto the grids in exactly the same way. Failure to observe these restrictions can lead to calculated energy differences several orders of magnitude too large. A common second calculation for the subtraction is to simply calculate the finite difference solution for the same charge distribution in a uniform dielectric of $\varepsilon_{\text{in}}$. For this case, an analytical solution of the finite difference equations is available, enabling significant computational savings (20).

Of course, the finite-difference method is not the only numerical method for solving the Poisson equation. The 3-D finite-*element* method also makes use of a mesh of points in three-dimensional space, but the points need not be regularly spaced. This allows for meshes that are customized to shapes of dielectric boundaries and the location of charges, finer mesh in regions of more interest, and so on. On the other hand, the algorithms are more complex and require more computation per mesh point than the finite difference method. Three-dimensional finite-element solvers specialized to molecular electrostatic applications have been developed (21,22) The Coulomb self-energy issue arises in the finite element method much as it does in the finite-difference method, and similar care with subtractions must be taken. Another numerical method is the boundary element method. It is specialized to systems with regions of uniform dielectric separated by sharp boundaries. The Poisson problem can then be recast into a self-consistency requirement between charges induced on the dielectric boundary elements and the electric field across the boundary. The Coulomb self energies appear as genuine singularities rather than finite artifacts of the numerical method, and they can simply be left out in practical calculations rather than arranging for them to be subtracted away. In principle of course, the rules at the end of Sec. 5 still apply. The surface element method has been adapted to molecular applications by several workers (23,24,25) including extension to the LPB equation (26).

## 7. SMALL-MOLECULE SOLVATION AND $\text{p}K_a$

The calculation of the electrostatic component of the solvation free energy of polar or charged molecules is closely related to the problem of calculating the energetics of protonation states, as well as being an important application of the MEAD model in its own right. The essential idea, illustrated in Figure 2, is to break the process of bringing a molecule from vacuum to solvent into three hypothetical steps: reduction to zero of the molecule's charges in vacuum; solvation of the purely non-polar molecule; and restoration of the original partial charges in the solvent environment. The overall solvation free energy is then,

$$\Delta G_{\text{sol}} = \Delta G_{\text{np}} - W_v + W_s, \quad (34)$$

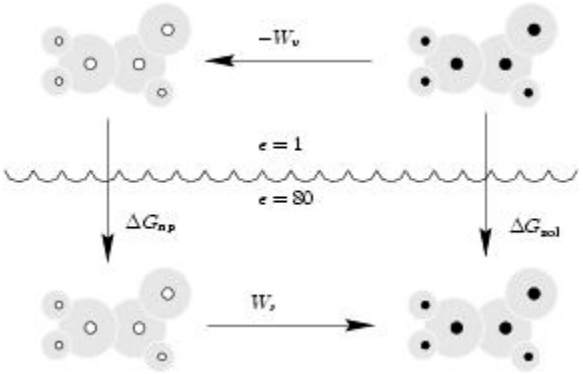


**Figure 2.** Thermodynamic cycle relating solvation free energy $\Delta G_{\text{np}}$ to the work of charging in solvent versus vacuum ($W_s$ versus $W_v$) and the free energy of solvating a sterically equivalent non-polar molecule $\Delta G_{\text{np}}$.

where $W_v$ and $W_s$ are the work of charging in the vacuum and solvent environment, respectively, and $\Delta G_{\text{np}}$ is the free energy of solvation of the hypothetical molecule with all partial charges set to zero. For some small molecules, the $\Delta G_{\text{np}}$ term can be estimated as the solvation energy of a sterically equivalent alkane. More often, empirical formulae relating $\Delta G_{\text{np}}$ to surface area and/or volume are used (27,28).

In the MEAD model for the work-of-charging calculations the solute molecule has an interior of dielectric constant $\varepsilon_{\text{in}}$ (typically 2 to account for electronic polarizability), the exterior has a dielectric constant of either 1 (for $W_v$) or 80 (for $W_s$ in water), and the boundary between the two dielectric regions is the molecular surface, as defined by Connolly (2). The difference calculation then obeys the rules set out at the end of Sec. 5 (the charges and interior dielectric calculations are the same in the two charging processes). From Eq. 31 and the cancellation of Coulombic terms it follows that

$$W_s - W_v = \frac{1}{2}\sum_i q_i \left(\phi_{r,s}(\mathbf{r}_i) - \phi_{r,v}(\mathbf{r}_i)\right), \qquad (35)$$

where $\phi_{r,s}$ and $\phi_{r,v}$ are the reaction potentials in solvent and vacuum, respectively. If the finite-difference method is used to solve the Poisson equation corresponding to the above MEAD model, the Coulombic contribution and the reaction-field contribution are both in the $\phi$ that is obtained from the grid, and the Coulomb $1/r$ singularities at the charge locations $\mathbf{r}_i$ are replaced by grid-dependent Coulombic artifacts. Provided that the finite-difference solutions for the potentials in solvent and vacuum, $\phi_s$ and $\phi_r$, are obtained using grids of the same spacing and the charges $q_i$ are mapped onto them in the same way in both calculations, the Coulomb contributions, including the grid artifacts will cancel, and we can use, as the practical expression for calculations,

$$W_s - W_v = \frac{1}{2}\sum_i q_i \left(\phi_s(\mathbf{r}_i) - \phi_v(\mathbf{r}_i)\right). \qquad (36)$$

This method has been shown to provide good accuracy for a wide variety of polar and charged solvents given a suitable parameterization of the atomic radii used to define the dielectric boundary, and the atomic partial charges (27,28).

A more rigorous approach treats the solute quantum mechanically, and demands self-consistency between the electronic structure and the reaction potential. Because electronic polarization is treated explicitly, $\varepsilon_{\text{in}}$ must be set to unity, and the reaction potential must be included in the quantum-mechanical Hamiltonian. The dependence of the reaction potential on the solute charge distribution and hence, the electronic structure, gives rise to the self-consistency requirement. The earliest applications of this idea date back to Onsager (29) who used a simplified spherical model. Application to more complex molecular shapes has been pioneered by Tomasi and co-workers (23,30) who used semi-empirical methods for electronic structure calculations, and a surface-element method to solve the Poisson equation. Extentions to ab initio quantum mechanics have also been made (31,32,30,33). The terms, polarized continuum model (PCM), or self-consistent reaction field (SCRF), are sometimes used to describe such calculations.

### 7.1. The Born model of ion solvation

If the geometry of the solute molecule is simply a sphere with a charge at the center, as in the case of a simple ion, the Poisson equation can be solved analytically. Consider a sphere with dielectric constant $\varepsilon_{\text{in}}$ inside and $\varepsilon_{\text{ex}}$ outside and a charge $q$ at the center. Because of spherical symmetry, the potential can only be a function of the distance $r$ from the sphere center. In the interior and exterior regions the Poisson equation is satisfied by

$$\phi_{\text{in}} = \frac{q}{\varepsilon_{\text{in}} r} + a \qquad (37)$$

$$\phi_{\text{ex}} = b\frac{q}{r} + c, \qquad (38)$$

where $a$, $b$ and $c$ are constants to be determined by boundary conditions. Since $\phi$ must go to zero as $r$ goes to infinity, $c = 0$. At the dielectric boundary, classical electrostatics (7) gives the boundary conditions that $\phi$ and the perpendicular component of the electric displacement $D_\perp = \varepsilon E_\perp$, must be continuous. That is,

$$\phi_{\text{in}}(R_B) = \phi_{\text{ex}}(R_B) \qquad (39)$$

$$\varepsilon_{\text{in}} \left.\frac{d\phi_{\text{in}}}{dr}\right|_{R_B} = \varepsilon_{\text{ex}} \left.\frac{d\phi_{\text{ex}}}{dr}\right|_{R_B}, \qquad (40)$$

where $R_B$ is the radius of the dielectric sphere. Substituting Eqs. 37 and 38 (with $c = 0$) leads to the solutions:

$$\phi_{\text{in}} = \frac{q}{\varepsilon_{\text{in}} r} + \frac{q}{R_B}\left(\frac{1}{\varepsilon_{\text{ex}}} - \frac{1}{\varepsilon_{\text{in}}}\right) \qquad (41)$$

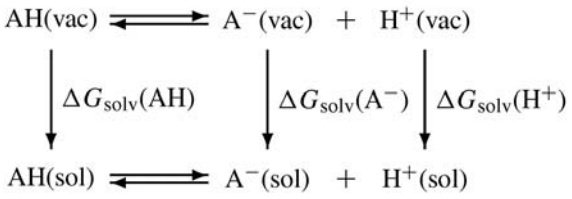


**Figure 3.** Cycle for absolute p$K_a$ calculations.

$$\phi_{\text{ex}} = \frac{q}{\varepsilon_{\text{ex}} r}. \qquad (42)$$

Note that $\phi_{\text{in}}$ has the expected separation into a Coulombic part (first term) and a reaction part, that in this case is simply a constant throughout the interior. Applying Eq. 35 or 36:

$$W_s - W_v = -\frac{q^2}{2R_B}\left(1 - \frac{1}{\varepsilon_{\text{ex}}}\right). \qquad (43)$$

This formula was first derived by Born using a somewhat different procedure (34).

### 7.2. Small molecule p$K_a$

Nearly all p$K_a$ calculations for ionizable groups in proteins are made with reference to model compounds of known p$K_a$, but for small molecules whose gas-phase proton affinity can be calculated by quantum chemical methods, an absolute p$K_a$ calculation is possible. Considering the cycle of Figure 3, one finds,

$$2.303RT\text{p}K_a = -\Delta G_{dg} - \Delta G_{\text{solv}}(\text{AH}) + \Delta G_{\text{solv}}(\text{A}^-) + \Delta G_{\text{solv}}(\text{H}^+). \qquad (44)$$

Here, the free energy of the dissociation reaction in the gas phase $\Delta G_{dg}$ is related to the proton affinity by the entropy of the liberated proton (26 eu) and a small correction ( 0 to 5 eu) for the entropy difference between A and AH. The solvation free energies of AH and A can be calculated by the methods of Sec. 7, but the $\Delta G_{\text{solv}}$ of a proton cannot. An experimental value for $\Delta G_{\text{solv}}(\text{H}^+)$ would depend on the absolute potential of the standard hydrogen electrode, which itself is only known approximately. On this basis, values of $\Delta G_{\text{solv}}(\text{H}^+)$ ranging from 259.5 to 262.5 kcal/mol have been suggested (35,36).

Lim *et al.* (35) explored the above approach to absolute p$K_a$ calculation using different charge and radius parameters. Because the magnitudes of $\Delta G_{dg}$ for small organic acids and bases range from 200–400 kcal/mol, and the solvation energies of the charged species are typically of order 100 kcal/mol, small percentage errors in the estimation of any of these terms can lead to substantial deviations from experimental p$K_a$ values (one p$K$ unit is equivalent to 1.4 kcal/mol at 300 K). Thus, Lim *et al.* found significant sensitivity to the choice of charge and radius parameters and to the details of solute geometry. An SCRF approach in which the geometry and solute charge is handled quantum mechanically leaves only atomic radii as empirical parameters, and yields reasonable estimates of p$K_a$ for a number of small organic molecules (31,37). The SCRF method has also been extended to p$K_a$ calculations of unusual species in protein active sites, such as a water molecule liganded to a manganese ion in superoxide dismutase (38). In this case, "solvation" means transfer from vacuum to an $\varepsilon_{\text{in}} = 1$ cavity within a protein active site, and the calculation must include the charges and dielectric constant of the remainder of the protein as well as the surrounding solvent dielectric. Facilities for the classical electrostatic part of such calculations are provided in the MEAD program suite.

## 8. PROTONATION STATES AND p$K_a$ IN PROTEINS

Rather than the more first-principles approach outlined in Sec. 7.2, calculations of protonation states and p$K_a$ values in proteins have generally used an approach based on model compounds of known p$K_a$, and electrostatic models to calculate shifts from the model compound values. Calculations of this general kind were introduced nearly 80 years ago by Linderstrøm-Lang (39) who modeled the protein as a sphere with the charges of the ionizable groups spread uniformly over its surface. As it become understood that proteins were not fluid globules but contained more specific structures, Tanford and Kirkwood (40,41) developed a model of protein ionizable sites as point charges uniformly spaced at a short fixed distance beneath the surface of a sphere. As actual protein structures became known, the Tanford–Kirkwood model was adjusted to use charge placements derived from the actual structures (42), and empirical corrections for differential solvent exposure were introduced (43,44).

The modern MEAD-based models described here (45), which have nearly displaced the sphere-based models, can be thought of as the natural extension of Tanford and Kirkwood's ideas to more detailed and realistic molecular surface shapes and charge distributions (Figure 4). However, several qualitatively new energy terms are included: the Born-like interaction of the ionizing group with the polarization that its ionization produces in the surroundings; and the interaction with non-ionizing groups in the protein, such as the backbone dipoles. In contrast, the Tanford–Kirkwood model only explicitly includes the electrostatic interactions between ionizing sites; the other terms, which could not have been explicitly calculated without more atomic detail, were left to be implicitly subsumed into the model compound p$K_a$.

The fundamental assumptions behind the methods described here are as follows: (1) The free energy of ionization can be divided into an internal part that includes bond breaking and other electronic structure changes and is confined to a relatively small number of atoms within the ionizing functional group, and an external part that includes interactions with the larger surroundings. (2) The internal part is the same for both the ionizing group in the protein and the corresponding model compound, but

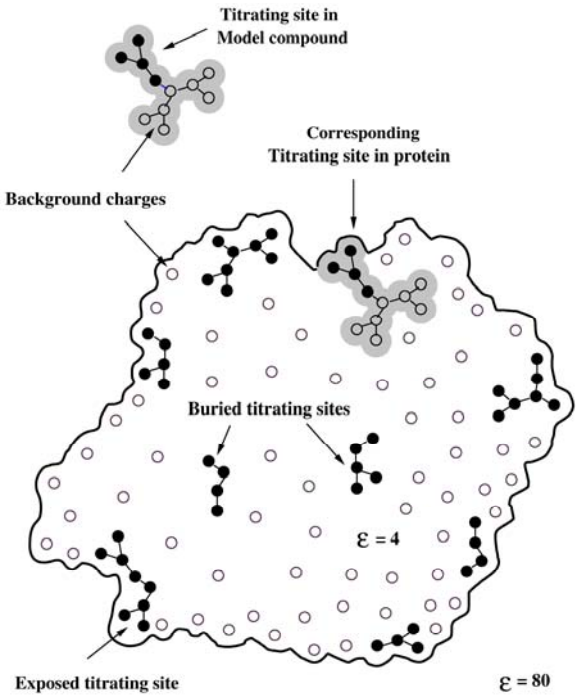


**Figure 4.** MEAD model for $pK_a$ calculations for proteins. The charges of the titrating site in protein or model compound (black circles in grey region) are changed from protonated to deprotonated values. Interactions occur with the site's own reaction potential; non-titrating polar groups in both the protein and model compound (open circles) and other ionizable groups in the protein (black circles in white areas).

the external part may differ. (3) Since the steric changes in protonation/deprotonation are subtle, and similar in both the protein and model compound the steric contribution to the difference of the external part can be neglected. (4) The remaining difference in the external part is purely electrostatic. (5) A MEAD model is adequate to describe this electrostatic difference. As a practical matter, other simplifying approximations are often introduced as well, such as neglect of conformational change and simplification of charge models; but these approximations can be lifted without changing the basic ideas.

### 8.1. One-site case

Consider a protein that contains only one ionizable chemical group, and suppose one wishes to calculate its $pK_a$ given the protein structure and $pK_{mod}$, the $pK_a$ of a small model compound containing that same chemical group. The one-site protein is a useful hypothetical construct because it removes the complication of interactions with other groups whose ionization states are pH dependent. In particular, we will adopt Tanford's definition of the "intrinsic $pK$" or $pK_{intr}$, as the $pK_a$ that a site in a protein would have if all other ionizable sites were held in some reference charge state, typically a neutral-charge state. We also neglect the conformational flexibility of the protein, except to the extent that it is included implicitly in the protein dielectric constant $\varepsilon_{in}$.

According to the fundamental assumptions listed above, the desired $pK_{intr}$ value is the $pK_{mod}$, modified by a suitable difference in electrostatic work of the protonated versus deprotonated states in the protein versus the model compound:

$$pK_{intr} = pK_{mod} - \frac{\left(W_p^{(p)} - W_p^{(d)}\right) - \left(W_m^{(p)} - W_m^{(d)}\right)}{2.303RT}, \qquad (45)$$

where the $W$ are the work of creating either the charge distribution of the protonated or deprotonated state ($(p)$ or $(d)$ superscripts) in the protein or the model compound ($p$ or $m$ subscripts). As discussed in Sec. 5, each of these work terms potentially contains contributions that go to infinity in the point-charge limit and care must be taken to ensure that these cancel in the final calculation. To this end, we begin with Eq. 30, in which the small-sphere energies that lead to these infinities is explicit, and we distinguish the small set of charges $Q$ that differ between the protonated and deprotonated and deprotonated states (filled circles in Figure 4) and the remaining charges $q$ (open circles) that do not. The result is:

$$\begin{aligned} W_p^{(p)} &= \sum_a \frac{Q_a^{(p)2}}{2\varepsilon_{in}R_a} + \sum_{ab,b<a} \frac{Q_a^{(p)}Q_b^{(p)}}{\varepsilon_{in}|\mathbf{r}_a - \mathbf{r}_b|} + \frac{1}{2}\sum_{ab} Q_a^{(p)}Q_b^{(p)} g_{r,p}(\mathbf{r}_a, \mathbf{r}_b) \\ &+ \sum_{ai} \frac{Q_a^{(p)} q_{p,i}}{\varepsilon_{in}|\mathbf{r}_a - \mathbf{r}_i|} + \sum_{ai} Q_a^{(p)} q_{p,i} g_{r,p}(\mathbf{r}_a, \mathbf{r}_i) \\ &+ \sum_i \frac{q_{m,i}^2}{2\varepsilon_{in}R_i} + \sum_{ij,j<i} \frac{q_{m,i}q_j}{\varepsilon_{in}|\mathbf{r}_i - \mathbf{r}_j|} + \frac{1}{2}\sum_{ij} q_{p,i}q_{p,j} g_{r,p}(\mathbf{r}_i, \mathbf{r}_j), \end{aligned} \qquad (46)$$

where the indices $a$ and $b$ label the titrating-group's charges, $i$ and $j$ label the non-titrating charges of the protein (the $q_p$), and $g_{r,p}$ is the reaction potential term of the Green function for the protein (see Eq. 28).

If the analogous expression for $W_p^{(d)}$ is written down and subtracted from the above, it is immediately seen that all terms involving interactions between the protein's non-titrating charges (the $qq$ terms) vanish. The interactions between titrating and non-titrating charges can be conveniently written down in terms of the potential due to the titrating charges, $\varphi_p(\mathbf{r}_j) = \sum_a Q_a g_p(\mathbf{r}_a, \mathbf{r}_j)$, where $g_p$ is the total green function (including the Coulombic part) for the protein, and superscripts can be added to the $Q$ and $\varphi_p$ to distinguish the ionization states as above. The difference between the two work terms is then,

$$\begin{aligned} W_p^{(p)} - W_p^{(d)} &= \sum_a \frac{Q_a^{(p)2} - Q_a^{(d)2}}{2\varepsilon_{in}R_a} + \sum_{ab,b<a} \frac{Q_a^{(p)}Q_b^{(p)} - Q_a^{(d)}Q_b^{(d)}}{\varepsilon_{in}|\mathbf{r}_a - \mathbf{r}_b|} \\ &+ \frac{1}{2}\sum_{ab} Q_a^{(p)}Q_b^{(p)} g_{r,p}(\mathbf{r}_a, \mathbf{r}_b) - \frac{1}{2}\sum_{ab} Q_a^{(d)}Q_b^{(d)} g_{r,p}(\mathbf{r}_a, \mathbf{r}_b) \\ &+ \sum_i q_{p,i}\left(\phi_p^{(p)}(\mathbf{r}_i) - \phi_p^{(d)}(\mathbf{r}_i)\right). \end{aligned} \qquad (47)$$

To complete the evaluation of the numerator in Eq. 45, an analogous expression for the work of the charge change in the model compound, $W_m^{(p)} - W_m^{(d)}$ must be subtracted from the above expression. This leads to a cancellation of all the Coulomb terms involving only the

titrating charges (the $QQ$ terms), including the small-sphere energies, so the problem of infinities in the point-charge limit is resolved. The resulting expression is:

$$\left(W_p^{(p)} - W_p^{(d)}\right) - \left(W_m^{(p)} - W_m^{(d)}\right) = \tag{48}$$
$$\frac{1}{2}\left[\sum_{ab} Q_a^{(p)} Q_b^{(p)} g_{r,p}(\mathbf{r}_a, \mathbf{r}_b) - \sum_{ab} Q_a^{(p)} Q_b^{(p)} g_{r,m}(\mathbf{r}_a, \mathbf{r}_b)\right]$$
$$-\frac{1}{2}\left[\sum_{ab} Q_a^{(d)} Q_b^{(d)} g_{r,p}(\mathbf{r}_a, \mathbf{r}_b) - \sum_{ab} Q_a^{(d)} Q_b^{(d)} g_{r,m}(\mathbf{r}_a, \mathbf{r}_b)\right]$$
$$+\sum_i q_{p,i}\left(\phi_p^{(p)}(\mathbf{r}_i) - \phi_p^{(p)}(\mathbf{r}_i)\right) - \sum_k q_{m,k}\left(\phi_m^{(p)}(\mathbf{r}_k) - \phi_m^{(p)}(\mathbf{r}_k)\right)$$

The reaction $QQ$ terms do not cancel, since the reaction part of the Green function is not the same in the protein as in the model compound. These terms can be written in the form $\sum_a Q_a \phi_r$, where $\phi_r$ is the reaction potential, as in Eq. 31. The expressions in the first set of square brackets is then $\sum_a Q_a^{(p)}(\phi_{r,p}^{(p)} - \phi_{r,m}^{(p)})$, and an analogous expression using the deprotonated charges is obtained for the second bracketed expression. These are very similar to Eq. 35 for the solvation case. The difference is, instead of altering the external dielectric environment from vacuum to solvent, we are altering the dielectric environment from that of a protein in solvent to that of the model compound in solvent. The rules at the end of Sec. 5 are satisfied as long is the titrating charges are in a region of dielectric $\varepsilon_{\text{in}}$ in both cases. Therefore, as in the discussion of solvation energy (see Eq. 36), we can substitute the finite-difference calculated potential due to the titrating charges for the reaction potentials to obtain a practical expression for calculations.

We have seen that Eq. 48 contains two distinct kinds of terms: the $QQ$ terms leading to expressions similar to those for electrostatic solvation energy; and the $q\phi$ (or $Qq$) terms corresponding to interactions of the titrating charges with the non-titrating background. It has become conventional to refer to these terms as the Born and and background terms, respectively. The expression for $\text{p}K_{\text{intr}}$ is then written:

$$\text{p}K_{\text{intr}} = \text{p}K_{\text{mod}} - \frac{\Delta\Delta G_{\text{Born}} + \Delta\Delta G_{\text{back}}}{RT \ln 10} \tag{49}$$

where,

$$\Delta\Delta G_{\text{Born}} = \frac{1}{2}\sum_a^{\text{titr}} Q_a^{(p)}\left(\phi_p^{(p)}(\mathbf{r}_a) - \phi_m^{(p)}(\mathbf{r}_a)\right) - Q_a^{(d)}\left(\phi_p^{(d)}(\mathbf{r}_a) - \phi_m^{(d)}(\mathbf{r}_a)\right) \tag{50}$$

$$\Delta\Delta G_{\text{back}} = \sum_i^{\text{protein}} q_{m,i}\left(\phi_p^{(p)}(\mathbf{r}_i) - \phi_p^{(d)}(\mathbf{r}_i)\right) - \sum_k^{\text{model}} q_{m,k}\left(\phi_m^{(p)}(\mathbf{r}_k) - \phi_m^{(d)}(\mathbf{r}_k)\right) \tag{51}$$

Note that the same four potentials are needed for both the Born and background term: the potentials generated by the titrating charges in both their protonated and deprotonated states in both the protein and the model compound. The potential generated by the non-titrating charges need not be calculated — the non-titrating charges enter the $\Delta\Delta G_{\text{back}}$ expression only as charges that "feel" the potential, not as charges that generate it.

It should be emphasized that the above is valid only if the titrating charges are the same in the protein and model compound and if the interatomic distances between them are the same. Further, if finite-difference or finite-element methods are used, the way that the numerical grid is set up around the titrating charges, and the way that the charges are distributed over them must be identical. When calculations of this kind were first introduced (45) a further precaution was taken along these lines: *all* the atomic charges positions and radii of the model compound, even "background" charges were made identical to corresponding atoms in the protein. In other words, the conceptual model of Figure 4, in which the model compound appears to be "cut out" from the protein, was followed strictly. This has the advantage of canceling some of the errors in the finite-difference method that tend to be more severe for interactions between near atoms, such as bonded pairs within the model compound. But it has the peculiarity that the calculations use a different model compound coordinate sets for each site, even for sites of the same residue type. Most subsequent calculations of this kind have followed a similar practice. However, schemes that include conformational flexibility of both protein sidechains and model compounds need not have this limitation (46).

### 8.2. Multiple interacting sites

In passing to the full model implied by Figure 4, we must include the electrostatic interactions between the ionizable groups. Strictly speaking, it is no longer possible to rigorously define the $\text{p}K_a$ of individual sites, so we shall first consider the relative energetics of different protonation states of the protein, and then the statistics of ensembles over the possible states. This leads to predictions of the degree of protonation of each site as a function of pH, and these pH dependencies can usually (but not always) be reasonably well described by a $\text{p}K_a$-like quantity.

By "protonation state" of the protein, we mean a specification of which sites are protonated and which are deprotonated. If the protein has $N$ sites, each with two possible protonation states, there are $2^N$ possible protonation states of the protein. Let them be denoted by the $N$-element vector, $\mathbf{x}$ whose elements $x_i$ take can each take on values representing "protonated" or "deprotonated." Let $0$ be a particular value of this vector chosen as a reference state, for example, the state with all sites in their neutral state, as in the definition of $\text{p}K_{\text{intr}}$. Consider the chemical equilibrium between some state $\mathbf{x}$ and the reference state:

$$\text{M}(0) + \nu(\mathbf{x})\text{H}^+ \rightleftharpoons \text{M}(\mathbf{x}) \tag{52}$$

where $\nu(\mathbf{x})$ is the number of protons that would be released on going from state $\mathbf{x}$ to the reference state. The free energy change for going to the right in this reaction at some fixed pH is,

$$\Delta G(\mathbf{x}, \text{pH}) = -RT \ln \frac{[\text{M}(\mathbf{x})]}{[\text{M}(0)]} = \mu_{\text{M}}^{\circ}(\mathbf{x}) - \mu_{\text{M}}^{\circ}(0) - \nu(\mathbf{x})(\mu_{\text{H}^+}^{\circ} - 2.303RT\,\text{pH}), \tag{53}$$

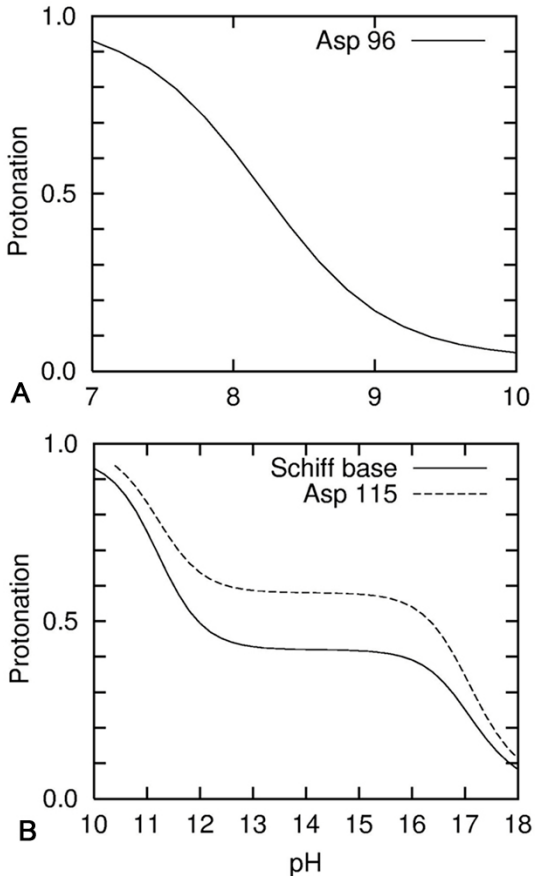


**Figure 5.** Titration curves of sites in Bacteriorhodopsin, taken from the work of ref. (17).

where the $\mu^\circ$ are standard chemical potentials.

Suppose $P_i(x_i)$ is the change in the protein's chemical potential for changing site $i$ from its reference state to state $x_i$, while all other sites remain in the reference state. The expression for chemical potential will then contain a sum of these $P_i$, but more terms are needed for the site–site interactions. Since the interactions are presumed to be governed by linear equations (the Poisson or LPB equations) these terms will be pairwise additive. Therefore,

$$\mu_M^\circ(\mathbf{x}) = \mu_M^\circ(0) + \sum_i^N P_i(x_i) + \frac{1}{2}\sum_{ij,i\neq j}^N W_{ij}(x_i,x_j), \qquad (54)$$

where $W_{ij}$ is the electrostatic interaction between sites $i$ and $j$, relative to the reference state. Inserting this into Eq. 53 and writing $\nu(\mathbf{x})$ as a sum over sites, $\sum_i \nu_i(x_i)$, gives,

$$\Delta G(\mathbf{x},\mathrm{pH}) = \sum_i [P_i(x_i) - \nu_i(x_i)(\mu_{\mathrm{H}^+}^\circ - 2.303RT\,\mathrm{pH})] + \frac{1}{2}\sum_{ij,i\neq j}^N W_{ij}(x_i,x_j) \quad (55)$$

Some consideration of the way in which $P$, $\nu$ and $\mathrm{p}K_{\mathrm{intr}}$ are defined in terms of a reference state leads to the the relation, $P_i(x_i) = \nu_i(x_i)(\mu_{\mathrm{H}^+} - 2.303RT\,\mathrm{p}K_{\mathrm{intr},i})$, so that,

$$\Delta G(\mathbf{x},\mathrm{pH}) = \sum_i \nu_i(x_i) 2.303RT(\mathrm{pH} - \mathrm{p}K_{\mathrm{intr},i}) + \frac{1}{2}\sum_{ij,i\neq j}^N W_{ij}(x_i,x_j). \qquad (56)$$

The intrinsic $\mathrm{p}K_a$ values of each site, $\mathrm{p}K_{\mathrm{intr},i}$, can be calculated by the methods of Sec. 8.1. The $W_{ij}(x_i,x_j)$ can be calculated by considering the additional electrostatic work to change site $i$'s charges from the reference state to $x_i$ if site $j$ is in state $x_j$ instead of its reference state. By this definition, $W_{ij}$ is non-zero only if both $x_i$ and $x_j$ are different from their standard states [3]. If, for example, the deprotonated states of both $i$ and $j$ are the standard states, then

$$W_{ij}(\mathrm{prot},\mathrm{prot}) = \sum_a^{\mathrm{site}\,i}\left(Q_a^{(p)} - Q_a^{(d)}\right)[\phi_j^{(p)}(\mathbf{r}_a) - \phi_j^{(d)}(\mathbf{r}_a)] \quad (57)$$
$$= \sum_b^{\mathrm{site}\,j}\left(Q_b^{(p)} - Q_b^{(d)}\right)[\phi_i^{(p)}(\mathbf{r}_b) - \phi_i^{(d)}(\mathbf{r}_b)],$$

where $\phi_i^{(p)}$ is the potential produced by the site $i$ charges in their protonated state, and so forth, and the sums run over the atoms of the indicated site. Note that the four different potentials needed here are are already available from the calculations of the intrinsic $\mathrm{p}K_a$ calculations for the two sites (Eqs. 49–51). Therefore the construction of a function that gives the relative energies of all $2^N$ possible protein protonation states requires just $4N$ solutions of the Poisson or LPB equation.

The pH-dependent protonation state free energy function, $\Delta G(\mathbf{x},\mathrm{pH})$ can be used to calculate probabilities of protonation states and averages of quantities depending on protonation state by formulae analogous to the canonical distribution of statistical mechanics. For example, the fraction of all protein M that is in state $\mathrm{M}(\mathbf{x})$ is

$$\frac{[\mathrm{M}(\mathbf{x})]}{[\mathrm{M}]} = \frac{\exp[-\Delta G(\mathbf{x},\mathrm{pH})/RT]}{Z(\mathrm{pH})}, \qquad (58)$$

where $Z$ is the normalization constant or partition function given by,

$$Z(\mathrm{pH}) = \sum_{\mathbf{x}}^{2^N} \exp[-\Delta G(\mathbf{x},\mathrm{pH})/RT] \qquad (59)$$

where the sum runs over all possible protonation states. Perhaps the most common average taken is the the average protonation of a particular site:

$$\theta_i(\mathrm{pH}) = \frac{1}{Z(\mathrm{pH})}\sum_{\mathbf{x}}^{2^N} \nu_i(x_i)\exp[-\Delta G(\mathbf{x},\mathrm{pH})/RT]. \quad (60)$$

Some illustrative plots of $\theta_i$ versus pH are shown in Figure 5. In most cases the curves are have an approximately Henderson–Hasselbalch form, as in Figure 5a. One can then define $\mathrm{p}K_{\mathrm{half}}$, a quantity roughly analogous to $\mathrm{p}K_a$, as the pH at which the plot crosses the protonation fraction, 0.5. But strong couplings between two sites titrating in overlapping pH ranges can lead to cases where $\mathrm{p}K_{\mathrm{half}}$ is nearly meaningless; instead the pivotal pH values are those that mark changes between no protons on either site, a single proton shared between the sites, and both sites protonated (Figure 5b). When three or more sites strongly couple, it is even possible to have the

counterintuitive result that one site may, within a limited pH range, *increase* in protonation as pH increases (17) a situation that has also been observed experimentally (48). The total protonation of all sites, however, must always monotonically decrease with increasing pH. Recently some methods of disentangling the complexities of multi-site titration curves have been presented by Onufriev *et al.* (49) Calculated titration curves often have unusual shapes for the active-site groups in proteins, because close proximity and, quite often, a solvent shielded environment give rise to strong site–site couplings. Recently, this has been used as a diagnostic to predict the location of protein active sites (50).

If there are no more than 12 to 15 sites, averages like $\theta_i$ can be evaluated directly from expressions like Eq. 60, but as the number of sites $N$ increases, the cost of evaluating the sums quickly becomes untenable. For such situations, several approximate methods are available. Rather than describe them in detail, we only outline them here, with citations to papers that provide more thorough descriptions.

**8.2.1. Tanford–Roxby approximation**

It is assumed that each site $i$ interacts not with particular protonation states of other sites, $j$ but with their (pH dependent) average protonation, $\theta_j$ (42). Tanford and Roxby's formulae can be derived from a mean-field approximation in which correlations between the protonation states of sites are neglected; and it can be shown that this approximation breaks down in cases where strongly coupled sites titrate in the same pH range (51).

**8.2.2. Reduced Site approximation**

For each pH value, a preliminary calculation is done to determine which sites can be regarded as almost completely protonated or almost completely deprotonated. These sites are then regarded as fixed in the protonated or deprotonated states, respectively, reducing the number of variable sites in the calculation (51). This approximation is quite accurate, except in the extreme-pH tails of the titration curves. However, in typical applications the effective number of sites is only cut by about half, so this method is useful only up to about 30 ionizable groups. The author's implementation of this method is part of the `MEAD` suite.

**8.2.3. Monte-Carlo Methods**

The application of Monte-Carlo methods to the multi-site titration problems was introduced by Beroza *et al.*(52) An initial protonation state is selected, then sites are flipped at random between the protonated and deprotonated states, and the flips are accepted or rejected based on the change in $\Delta G(\mathbf{x},\mathrm{pH})$ resulting from the flip. A two-site flipping strategy may be needed to obtain convergence for strongly coupled sites. The computational cost is a polynomial in $N$ rather than an exponential, so it is usable in practice for systems containing hundreds of sites. The method is reasonably accurate if applied correctly, although the titration curves produced are somewhat "noisy." Beroza's implementation of the method (52,47) is available on the Internet (ftp://ftp.scripps.edu/case/beroza)

**8.2.4. Clustering methods**

Variants of this idea have been introduced by several authors (53,54,55). The idea is that in calculating the protonation of site $i$, one can use a mean-field approximation for weakly coupled or distant sites, and more exact expressions for the strongly coupled (or nearby) ones. The version of this idea developed in the author's group is called Iterative Mobile Clustering (IMC) and has been described in detail and tested in a recent paper (55). This method is also applicable to multi-conformational problems. A general purpose implementation of IMC is planned, but not yet written.

Tautomerism of sidechains such as histidine can be incorporated into the above formalism by allowing the $x_i$ to take on appropriate values, such as "epsilon," "delta" and "protonated." In that case, six Poisson or LPB solutions would be required for each histidine residue so treated. (Calculations incorporating tautomerism in essentially this way were first done nearly a decade ago (56), but since the two-state "protonated/deprotonated" scheme was hard-wired in the software at that time, an equivalent scheme using extra pseudo-sites was devised. This trick has been described in detail by Baptista *et al.* (57).) It is also possible to incorporate the binding of other ions to specific sites, or oxidation-state changes into the above formalism. This allows one to calculate, for example, the pH dependence of redox potentials in proteins or the workings of energy transduction proteins in which electron and proton transfer are coupled (58,59,60). Ref. (55) provides an extension of the above formal framework that covers both tautomerism, binding of other ligands and redox changes.

**8.3. Conformational Flexibility**

The above methods do not allow for conformational flexibility, except implicitly through the protein dielectric constant. But since the dielectric response of the protein is supposed to be within the linear regime, this implicit flexibility cannot involve much more than modest localized fluctuations of dipoles. Significant global conformational changes, such as unfolding or hinge-bending, go unrepresented. Even changes confined to a few sidechain degrees of freedom, such as the formation or breaking of salt bridges, cannot be plausibly subsumed into the dielectric response, especially insofar as they affect the $\mathrm{p}K_a$ values of the sidechains themselves. One should therefore expect the method to break down in cases where conformational changes have a significant influence on $\mathrm{p}K_a$.

The prediction of extreme $\mathrm{p}K_a$ values should be taken as a possible indicator of such a breakdown. For example, in the earliest calculations of this kind (45), a $\mathrm{p}K_a$ of around 20 was calculated for Tyr53 of lysozyme. However, the unfolding of lysozyme is known to be coupled to the ionization of this residue (at pH 12). The high calculated number should be understood as the $\mathrm{p}K_a$ that the site would have if the protein could somehow be constrained to stay near its native conformation at very high pH. On the other hand, some residues do have

functionally important large p$K$ shifts that are correctly predicted by the methods. Examples include bacteriorhodopsin (17) and protein tyrosine phosphatase (61), though in some cases the method over-predicts the magnitude of the shift.

The most desirable solution, in principle, is to include conformational flexibility explicitly in the calculation. However, this raises complex problems. The free energy change associated with changing conformational states now becomes part of the problem, and this includes many non-electrostatic factors. For example, in the alkaline denaturation example, the p$K_a$ becomes higher to the extent that the forces stabilizing the native state, such as van der Waals and hydrophobic interactions, resist the driving force for alkaline denaturation, which is proportional to the difference between the pH and the p$K_a$ that the still-protonated sites would have in the unfolded state. For practical calculations including flexibility, the number of conformers that should be included, and how they should be selected is far from obvious. For a fairly complete formulation emphasizing the problem of enumerating the conformational states and considering the correlations between distinct flexible regions of a protein, see Ref. (55). Development of methods to include conformational flexibility in titration calculations has been a topic of active research using a number of different approaches (46,47,62-68), and will not be reviewed in detail here.

However, we will present one easily implemented method based on integration over binding isotherms. It is quite useful for the case of pH-driven unfolding (69), and it has also been applied to electron transfer (58). It can be shown (70,71,72) that the pH dependence of the free energy of a conformational change from A to B can be expressed as

$$\Delta G_{AB}(\mathrm{pH}) - \Delta G_{AB}(\mathrm{pH}_\circ) = 2.302RT\int_{\mathrm{pH}_\circ}^{\mathrm{pH}} [Q_B(pH') - Q_A(pH')]\, dpH', \quad (61)$$

where the $Q$ are either the total charge or total number of protons in the protein bound in state A or B. The integrands can be calculated by the methods of Sec. 8.2 given structural models for conformers A and B. Or, if one of the conformers is the unfolded state, one might assume that its residues titrate like independent sites with p$K_a$'s equal to the p$K_{\mathrm{mod}}$ values (69). Having $\Delta G_{AB}$ at any one pH allows its value at any other pH to be calculated, in principle. For example, if the pH for acid unfolding (where $\Delta G_{AB} = 0$) is known, then the stability of the protein at neutral pH can be calculated. In effect, the problem of knowing the non-electrostatic contributions to the conformational energetics has been subsumed into the need to know $\Delta G_{AB}$ at a particular pH. Titration curves for individual sites (the $\theta_i$) can be obtained in a way that accounts for the conformational change by weighting the contributions from the A-conformer and the B-conformer in calculations of $\theta_i$ according to $\Delta G_{AB}(\mathrm{pH})$, at each pH point.

## 9. OPEN PROBLEMS

That electrostatic effects are the primary means by which the protein environment modifies the $H^+$-titration properties of its ionizable groups is beyond dispute, but one can certainly question whether the approximations of macroscopic electrostatics are permissable in the calculation of such effects, and if so, what macroscopic parameters, such as dielectric constants and boundary definitions, ought to be used. MEAD models seem to be on fairly good ground in at least one area: the treatment of solvent water as a region of high dielectric. Calculations of small molecule solvation energies by the methods of Sec. 7 have been quite successful, given some modest efforts at parameterization (27,28,36,73). Comparisons between molecular dynamics-based thermodynamics calculation using an atomistic representation of both solvent and solute, and a MEAD model of solvation and H-bonding show that the two give very similar results, at least when the the standard, low-cost atomic models of solvent, such as TIP3P are used for small molecules whose charges are no more than monovalent(74,75).

The depiction of the protein as a macroscopic dielectric medium is another matter. Theories that connect microscopic models to a macroscopic dielectric assume an orders-of-magnitude separation between the microscopic length scale and the size of any region to which a dielectric constant is assigned. Proteins are in a mesoscopic grey zone, in that the characteristic protein distance (the protein radius, say) is only a few times greater than the length scale of the microscopic dipolar elements it contains (e. g., backbone amides). Furthermore, proteins do not appear to be particularly uniform within their interior. There has been some suggestion of addressing the non-uniformity problem by assigning different dielectric constants to different parts of the protein (76), but since these parts must necessarily be smaller than the protein, the microscopic/mesoscopic problem alluded to above is exacerbated. Some workers (77) have criticized the protein dielectric idea as invalid, particularly when the dipoles whose fluctuations constitute the dielectric response are also present in the calculations, as in Eq. 51. As an alternative, they advocate an approach that resembles the standard microscopic molecular dynamics approaches, but enforces linear response and modifies electrostatic terms according to a scaling factor in such a way that the resulting model appears quite similar, in effect, to a MEAD model (78).

Recently, a series of papers by Simonson and co-workers have presented some careful analysis of the relationship between microscopic and macroscopic representations of protein electrostatics. They performed microscopic calculations of the response of the protein medium to the insertion of a charge at various locations in the protein interior and found that these were well matched by a macroscopic model with a uniform dielectric constant in the protein region (79). The best value of the dielectric constant for such a match was in close agreement with that calculated using a modified version of Kirkwood–Fröhlich theory to relate protein dipole fluctuations in a microscopic protein/water simulation to the protein dielectric constant (80-84). This finding of consistency between various ways of relating microscopic fluctuations and responses to

macroscopic dielectric theory provides some support for the extension of macroscopic ideas to proteins.

Even if the idea of a protein dielectric constant is acceptable, there remains the question of its value. Many early workers in the field, following the suggestion of Tanford and co-workers (41,42) used values near 4, which is consistent with measurements on dry protein powders (85,86). Early molecular mechanics calculations using Kirkwood–Fröhlich theory (80,81) to calculate the dielectric constant from microscopic dipole fluctuations supported similar values (87,88). More recent calculations, in which increased computing power allows explicit solvent to be included, seemed at first to suggest higher values of the protein dielectric constant, such as 20 to 35, but more detailed analysis showed that the large dipole fluctuations were mainly due to the mobility charged sidechains at the protein surface. If only the more buried polar groups are considered, much lower values, such as 2 to 6, are calculated (82,83,84,89).

Antosiewicz *et al.* have taken a more empirical approach to the protein dielectric question (90,91). For a set of proteins for which the $pK_a$ of a number of sidechains was known experimentally, they made calculations by the methods of Sec. 8 using various values of $\varepsilon_{in}$ and found that the root mean square error was minimized with $\varepsilon_{in} \approx 20$. In the present author's view, the counter-argument is as follows: Most ionizable groups are on the protein surface where they are well exposed to solvent or can become so with a sidechain conformational change, and their $pK_a$ values are only slightly shifted from those of model compounds. Standard single-conformer MEAD models tend to overestimate these shifts because the lack of conformational flexibility eliminates a relaxation mechanism that would allow for more "normal" calculated titration properties. Raising $\varepsilon_{in}$ to high values tends to minimize broad statistical measures of error simply because it tends to make calculated shifts smaller. However, important active-site residues are often unusual in that they have large $pK_a$ shifts, and a computational method that tends to scale down all shifts risks missing these. Indeed, we have computed several large, functionally important, $pK_a$ shifts in proteins that could not have been predicted with a high $\varepsilon_{in}$ value (17,61,92,93).

Krishtalik *et al.* (94) have made an interesting proposal to address the potential inconsistency (77) of explicit inclusion of peptide dipoles when these same dipoles' fluctuations are treated implicitly as a dielectric response. To state the problem as it relates to $pK_a$ calculations, consider the one-site problem of Sec. 8.1. The incremental work of adding an incremental charge to the site is $\delta W = \delta q(\langle V_\circ \rangle + \langle \Delta V \rangle)$, where $\langle V_\circ \rangle$ is the average electrostatic potential at the site due to all other charges, including protein dipoles, prior to any charge at the site, and $\langle \Delta V \rangle$ is the average change in that potential due to the protein and solvent dipole's reorientation in response to the site's developing charge. Macroscopic calculations of $\Delta\Delta G_{Born}$ (Eq. 50) correspond well to the $\langle \Delta V \rangle$ term, as shown by comparison to microscopic charging calculations (79). However, it can be argued that for the calculation of $\Delta\Delta G_{back}$, which should correspond to the the $\langle V_\circ \rangle$ term, the use of a protein dielectric higher than the optical dielectric constant ($\approx 2$) constitutes a sort of double counting because the coordinates in the calculation already reflect the orientational polarization of the protein. Thus, it is suggested that a low protein dielectric constant (1–2) should be used for the $\Delta\Delta G_{back}$ term while a higher dielectric constant ($\geq 3$) may be used for $\Delta\Delta G_{Born}$ to reflect the changing orientational polarization as the charge develops. This would appear to introduce an inconsistency of its own — the use of two different dielectric constants for one and the same material during the same charging process — but a consistent scheme for implementing this idea has been devised (95). It requires a detailed microscopic model for the whole protein both before and after the charge change at the site, and is therefore considerably more complicated to implement, particularly for a multi-site problem.

Many of the problems and ambiguities outlined above can in principle be removed or ameliorated by a proper treatment of conformational flexibility (Sec. 8.3). Although the formalism and the means to overcome some combinatorial problems have been developed (55), a good general method to generate the important conformers without creating an unmanageably large number of them has yet to be developed. In this connection, workers in the field might do well to look at the remarkable progress being made in handling the combinatorics of sidechain conformers in the field of protein design (96,97,98).

## 10. REFERENCES


1. Warwicker, J. & H. C. Watson: Calculation of the electric potential in the active site cleft due to $\alpha$-helix dipoles. *J Mol Biol* 157, 671–679 (1982)
2. Connolly, M. L.: Solvent-accessible surfaces of proteins and nucleic acids. *Science* 221, 709–713 (1983)
3. Richards, F. M.: Areas, volumes, packing and protein structure. *Ann Rev Biophys Bioeng* 6, 151–176 (1977)
4. Honig, B. & A. Nicholls: Classical electrostatics in biology and chemistry. *Science* 268, 1144–1149 (1995)
5. Juffer, A. H.: Theoretical calculations of acid-dissociation constants of proteins. *Biochem Cell Biol* 76, 198–209 (1998)
6. GNU general public license, version 2. Published by The Free Software Foundation, 675 Massachusetts Ave., Cambridge, MA 02139, USA (1991)
7. Jackson, J. D.: Classical Electrodynamics. Wiley and Sons, New York, 2 edn. (1975)
8. McQuarrie, D. A.: Statistical Mechanics. Harper and Row, New York (1976)
9. Debye, P. & E. Hückel: *Phys Z* 24, 185 (1923)
10. Chandler, D.: Introduction to Modern Statistical Mechanics. Oxford, New York (1987)
11. Gilson, M. K., K. A. Sharp & B. Honig: Calculating the electrostatic potential of molecules in solution: Method and error assessment. *J Comp Chem* 9, 327–335 (1987)
12. Mohan, V., M. E. Davis, J. A. McCammon & B. M. Pettitt: Continuum model calculations of solvation free

energies: Accurate evaluation of electrostatic contributions. *J Phys Chem* 96, 6428–6431 (1992)
13. Beroza, P. & D. R. Fredkin: Calculation of amino acid p$K_a$ s in a protein from a continuum electrosatic model: Method and sensititivity analysis. *J Comp Chem* 17, 1229–1244 (1996)
14. Press, W. H., B. P. Flannery, S. A. Teukolsky & W. T. Vetterling: Numerical Recipes. The Art of Scientific Computing. Cambridge University Press, Cambridge (1986)
15. Briggs, W. L.: A Multigrid Tutorial. SIAM, Philadelphia (1987)
16. Hackbusch, W.: Iterative Solutions of Large Sparse Systems of Equations, vol. 95 of *Applied Mathematical Sciences*. Springer, New York (1994)
17. Bashford, D. & K. Gerwert: Electrostatic calculations of the p$K_a$ values of ionizable groups in bacteriorhodopsin. *J Mol Biol* 224, 473–486 (1992)
18. Bashford, D.: An object-oriented programming suite for electrostatic effects in biological molecules. In: Scientific Computing in Object-Oriented Parallel Environments, Eds. Ishikawa, Y., R. R. Oldehoeft, J. V. W. Reynders & M. Tholburn, ISCOPE97, Springer, Berlin (1997), vol. 1343 of *Lecture Notes in Computer Science*, 233–240
19. Nicholls, A. & B. Honig: A rapid finite difference algorithm, utilizing successive over-relaxation to solve the Poisson-Boltzmann equation. *J Comp Chem* 12, 435–445 (1991)
20. Luty, B. A., M. E. Davis & J. A. McCammon: Electrostatic energy calculations by a finite-difference method: Rapid calculation of charge–solvent interaction energies. *J Comp Chem* 6, 768–771 (1992)
21. You, T. J. & S. C. Harvey: Finite-element approach to the electrostatics of macromolecules with arbitrary geometries. *J Comp Chem* 14, 484–501 (1993)
22. Cortis, C. M., J.-M. Langlois, M. D. Beachy & R. A. Friesner: Quantum mechanical geometry optimization in solution using a finite element continuum electrostatics method. *J Chem Phys* 105, 5472–5484 (1996)
23. Miertus, S., E. Scrocco & J. Tomasi: Electrostatic interaction of a solute with a continuum: A direct utilization of *ab initio* molecular potentials for the prevision of solvent effects. *Chem Phys* 55, 117–129 (1981)
24. Zauhar, R. J. & R. S. Morgan: *J Mol Biol* 186, 815 (1985)
25. Zauhar, R. J. & A. Varnek: A fast and space-efficient boundary element method for computing electrostatic and hydration effects in large molecules. *J Comp Chem* 17, 864–877 (1996)
26. Boschitsch, A. H., M. O. Fenley & H.-X. Zhou: Fast boundary element method for the linear Poisson–Boltzmann equation. *J Phys Chem B* 106, 2741–2754 (2002)
27. Sitkoff, D., K. A. Sharp & B. Honig: Accurate calculation of hydration free energies using macroscopic solvent models. *J Phys Chem* 98, 1978–1988 (1994)
28. Nina, M., D. Beglov & B. Roux: Atomic radii for continuum electrostatics calculations based on molecular dynamics free energy simulations. *J Phys Chem B* 101, 5239–5248 (1997)
29. Onsager, L.: Electric moments of molecules in liquids. *J Amer Chem Soc* 58, 1486–1493 (1936)
30. Tomasi, J. & M. Persico: Molecular interactions in solution: An overview of methods based on continuous distributions of the solvent. *Chem Rev* 94, 2027–2094 (1994)
31. Chen, J. L., L. Noodleman, D. A. Case & D. Bashford: Incorporating solvation effects into density functional electronic structure calculations. *J Phys Chem* 98, 11059–11068 (1994)
32. Tannor, D. J., B. Marten, R. Murphy, R. A. Friesner, D. Sitkoff, A. Nicholls, M. Ringnalda, W. A. Goddard, III & B. Honig: Accurate first principles calculation of molecular charge distributions and solvation energies from ab initio quantum mechanics and continuum dielectric theory. *J Am Chem Soc* 116, 11875–11882 (1994)
33. Tuñón, I., M. F. Ruiz-López, D. Rinaldi & J. Bertrán: Compuation of hydration free energies using a parameterized continuum model: Study of equilibrium geometries and reactive processes in water solution. *J Comp Chem* 17, 148–155 (1996)
34. Born, M.: Volumes and heats of hydration of ions. *Z Phys* 1, 45–48 (1920)
35. Lim, C., D. Bashford & M. Karplus: Absolute p$K_a$ calculations with continuum dielectric methods. *J Phys Chem* 95, 5610–5620 (1991)
36. Gilson, M. K. & B. Honig: Calculation of the total electrostatic energy of a macromolecular system: Solvation energies, binding energies, and conformational analysis. *Proteins* 4, 7–18 (1988)
37. Richardson, W. H., C.-Y. Peng, D. Bashford, L. Noodleman & D. A. Case: Incorporating solvation effects into density functional theory: Calculation of absolute acidities. *Int J Quant Chem* 61, 207–217 (1997)
38. Fisher, C. L., J.-L. Chen, J. Li, D. Bashford & L. Noodleman: Density-functional and electrostatic calculations for a model of a manganese superoxide dismutase active site in aqueous solution. *J Phys Chem* 100, 13498–13505 (1996)
39. Linderstrøm-Lang, K.: On the ionisation of proteins. *Comptes-rend Lab Carlsberg* 15, 1–29 (1924)
40. Tanford, C. & J. G. Kirkwood: Theory of protein titration curves. I. General equations for impenetrable spheres. *J Am Chem Soc* 79, 5333–5339 (1957)
41. Tanford, C.: Theory of protein titration curves. II. Calculations for simple models at low ionic strength. *J Am Chem Soc* 79, 5340–5347 (1957)
42. Tanford, C. & R. Roxby: Interpretation of protein titration curves. *Biochemistry* 11, 2192–2198 (1972)
43. Shire, S. J., G. I. H. Hanania & F. R. N. Gurd: Electrostatic effects in myoglobin. hydrogen ion equilibria in sperm whale ferrimyoglobin. *Biochemistry* 13, 2967–2974 (1974)
44. Matthew, J. B. & F. R. N. Gurd: Calculation of electrostatic interactions in proteins. *Meth Enzymol* 130, 413–436 (1986)
45. Bashford, D. & M. Karplus: p$K_a$ 's of ionizable groups in proteins: Atomic detail from a continuum electrostatic model. *Biochemistry* 29, 10219–10225 (1990)
46. You, T. & D. Bashford: Conformation and hydrogen ion titration of proteins: A continuum electrostatic model with conformational flexibility. *Biophys J* 69, 1721–1733 (1995)

47. Beroza, P. & D. A. Case: Including side chain flexibility in continuum electrostatic calculations of protein titration. *J Phys Chem* 100, 21056–20163 (1996)
48. Sudmeier, J. L. & C. N. Reilley: Nuclear magnetic resonance studies of protonation of polyamine and aminocoboxylate compounds in aqueous solution. *Analytical Chemistry* 36, 1698–1706 (1964)
49. Onufriev, A., D. A. Case & G. M. Ullmann: A novel view of pH titration in biomolecules. *Biochem* 40, 3413–3419 (2001)
50. Ondrechen, M. J., J. G. Clifton & D. Ringe: THEMATICS: A simple computational predictor of enzyme function from structure. *Proc Natl Acad Sci USA* 98, 12473–12478 (2001)
51. Bashford, D. & M. Karplus: Multiple-site titration curves of proteins: An analysis of exact and approximate methods for their calculation. *J Phys Chem* 95, 9556–9561 (1991)
52. Beroza, P., D. R. Fredkin, M. Y. Okamura & G. Feher: Protonation of interacting residues in a protein by Monte Carlo method: Application to lysozyme and the photosynthetic reaction center of *Rhodobacter sphaeroides*. *Proc Natl Acad Sci USA* 88, 5804–5808 (1991)
53. Gilson, M. K.: Multiple-site titration and molecular modeling: Two rapid methods for computing energies and forces for ionizable groups in proteins. *Proteins* 15, 266–282 (1993)
54. Yang, A.-S., M. R. Gunner, R. Sampogna, K. Sharp & B. Honig: On the calculations of p$K_a$s in proteins. *Proteins* 15, 252–265 (1993)
55. Spassov, V. Z. & D. Bashford: Multiple-site ligand binding to flexible macromolecules: Separation of global and local conformational change and an iterative mobile clustering approach. *J Comp Chem* 20, 1091–1111 (1999)
56. Bashford, D., D. A. Case, C. Dalvit, L. Tennant & P. E. Wright: Electrostatic calculation of side-chain p$K_a$ values in myoglobin and comparison with NMR data for histidines. *Biochemistry* 32, 8045–8056 (1993)
57. Baptista, A. M. & C. M. Soares: Some theoretical and computational aspects of the inclusion of proton isomerism in the protonation equilibrium of proteins. *J Phys Chem B* 105, 293–309 (2001)
58. Beroza, P., D. R. Fredkin, M. Y. Okamura & G. Feher: Electrostatic calculations of amino-acid titration and electron-transfer, $Q(A)^- Q(B) \rightarrow Q(A)Q(B)^-$, in the reaction-center. *Biophys J* 68, 2233–2250 (1995)
59. Alexov, E. G. & M. R. Gunner: Calculated protein and proton motions coupled to electron transfer from $Q_A^-$ to $Q_B^-$ in bacterial reaction centers. *Biochemistry* 38, 8253–8270 (1999)
60. Baptista, A. M., P. J. Martel & C. A. Soares: Simluation of electron-proton coupling with a Monte Carlo method: Application to cytochrome $c_3$ using continuum electrostatics. *Biophys J* 76, 2978–2998 (1999)
61. Dillet, V., R. L. Van Etten & D. Bashford: Stabilization of charges and protonation states in the active site of the protein tyrosine phosphatases: A compuational study. *J Phys Chem B* 104, 11321–11333 (2000)
62. Ripoll, D. R., Y. N. Vorobjev, A. Liwo, J. A. Vila & H. A. Scheraga: Coupling between folding and ionization equilibria: Effects of pH on the conformational preferences of polypeptides. *J Mol Biol* 264, 770–783 (1996)
63. Zhou, H.-X. & M. Vijayakumar: Modeling of protein conformational fluctuations in p$K_a$ predictions. *J Mol Biol* 267, 1002–1011 (1997)
64. Baptista, A. M., P. J. Martel & S. B. Petersen: Simulation of protein conformational freedom as a function of pH: constant-pH molecular dynamics using implicit titration. *Proteins* 27, 523–44 (1997)
65. Luo, R., M. Head, J. Moult & M. K. Gilson: p$K_a$ shifts in small molecules and HIV protease: Electrostatics and conformation. *J Am Chem Soc* 120, 6138–6146 (1998)
66. van Vlijmen, H. W. T., M. Schaefer & M. Karplus: Improving the accuracy of protein p$K_a$ calculations: Conformational averaging versus the average structure. *Proteins* 33, 145–158 (1998)
67. Nielsen, J. E. & G. Vriend: Optimizing the hydrogen-bond network in Poisson–Boltzmann equation-based p$K_a$ calculations. *Proteins* 43, 403–412 (2001)
68. Georgescu, R. E., E. G. Alexov & M. R. Gunner: Combining conformational flexibility and continuum electrostatics for calculating p$K_a$s in proteins. *Biophys J* 83, 1731–1748 (2002)
69. Yang, A.-S. & B. Honig: Structural origins of pH and ionic strength effects on protein stability. Acid denaturation of sperm whale apomyoglobin. *J Mol Biol* 237, 602–614 (1994)
70. Wyman, J.: Linked functions and reciprocal effects in hemoglobin. A second look. *Adv Prot Chem* 19, 223–286 (1964)
71. Tanford, C.: Protein denaturation. C. theoretical models for the mechanism of denaturation. *Adv Protein Chem* 24, 1–95 (1970)
72. Schellman, J. A.: Macromolecular binding. *Biopolymers* 14, 999–1018 (1975)
73. Sharp, K. A., A. Jean-Charles & B. H. Honig: A local dielectric constant model for solvation free energies which accounts for solute polarizability. *J Phys Chem* 96, 3822–3828 (1992)
74. Jayaram, B., R. Fine, K. Sharp & B. Honig: Free energy calculations of ion hydration: An analysis of the Born model in terms of microscopic simulations. *J Phys Chem* 93, 4320–4327 (1989)
75. Ösapay, K., W. S. Young, D. Bashford, C. L. Brooks, III & D. A. Case: Dielectric continuum models for hydration effects on peptide conformational transitions. *J Phys Chem* 100, 2698–2705 (1996)
76. Honig, B., K. Sharp & A.-S. Yang: Macroscopic models of aqueous solutions: Biological and chemical applications. *J Phys Chem* 97, 1101–1109 (1993)
77. King, G., F. S. Lee & A. Warshel: Microscopic simulations of macroscopic dielectric constants of solvated proteins. *J Chem Phys* 95, 4366–4377 (1991)
78. Sham, Y. Y., Z. T. Chu & A. Warshel: Consistent calculations of p$K_a$'s of ionizable residues in proteins: Semi-macroscopic and microscopic approaches. *J Phys Chem B* 101, 4458–4472 (1997)

79. Simonson, T. & D. Perahia: Microscopic dielectric properties of cytochrome *c* from molecular dynamics simulations in aqueous solution. *J Am Chem Soc* 117, 7987–8000 (1995)
80. Kirkwood, J. G.: *J Chem Phys* 7, 911 (1939)
81. Fröhlich, H.: Theory of Dielectrics. Oxford, 2 edn. (1958)
82. Simonson, T. & D. Perahia: Internal and interfacial dielectric properties of cytochrome *c* from molecular dynamics in aqueous solution. *Proc Natl Acad Sci U S A* 92, 1082–1086 (1995)
83. Simonson, T. & C. L. Brooks III: Charge screening and the dielectric constant of proteins: Insights from molecular dynamics. *J Amer Chem Soc* 118, 8452–8458 (1996)
84. Simonson, T.: Dielectric relaxation in proteins: Microscopic and macroscopic models. *Int J Quantum Chem* 73, 45–57 (1999)
85. Bone, S. & R. Pethig: Dielectric studies of the binding of water to lysozyme. *J Mol Biol* 157, 571–575 (1982)
86. Bone, S. & R. Pethig: Dielectric studies of protein hydration and hydration-induced flexibility. *J Mol Biol* 181, 323–326 (1985)
87. Gilson, M. K. & B. H. Honig: The dielectric constant of a folded protein. *Biopolymers* 25, 1097–2119 (1986)
88. Nakamura, H., T. Sakamoto & A. Wada: A theoretical study of the dielectric constant of protein. *Protein Engineering* 2, 177–183 (1988)
89. Smith, P. E., R. M. Brunne, A. E. Mark & W. F. van Gunsteren: Dielectric properties of trypsin inhibitor and lysozyme calculated from molecular dynamics simulations. *J Phys Chem* 97, 2009–2014 (1993)
90. Antosiewicz, J., J. A. McCammon & M. K. Gilson: Prediction of pH-dependent properties of proteins. *J Mol Biol* 238, 415–436 (1994)
91. Antosiewicz, J. & M. K. Gilson: The determinants of p $K_a$ s in proteins. *Biochemistry* 35, 7819–7833 (1996)
92. Demchuk, E., U. K. Genick, T. T. Woo, G. E. D. & B. Donald: Protonation states and pH titration in the photocycle of photoactive yellow protein. *Biochemistry* 39, 1100–1113 (2000)
93. Spassov, V. Z., H. Luecke, K. Gerwert & D. Bashford: p $K_a$ calculations suggest storage of an excess proton in a hydrogen-bonded water network in bacteriorhodopsin. *J Mol Biol* 312, 203–219 (2001)
94. Krishtalik, L. I., A. M. Kuznetsov & E. L. Mertz: Electrostatics of proteins: Description in terms of two dielectric constants simultaneously. *Proteins* 28, 174–182 (1997)
95. Simonson, T., G. Archontis & M. Karplus: A Poisson–Boltzmann study of charge insertion in an enzyme active site: The effect of dielectric relaxation. *J Phys Chem B* 103, 6142–6156 (1999)
96. Gordon, D. B. & S. L. Mayo: Radical performance enhancements for combinatorial optimization algorithms based on the dead-end elimination theorem. *J Comp Chem* 19, 1505–1514 (1998)
97. Looger, L. L. & H. W. Hellinga: Generalized dead-end elimination algorithms make large-scale protein side-chain structure prediction tractable: Implications for protein design and structural genomics. *J Mol Biol* 307, 429–445 (2001)
98. Desmet, J., J. Spriet & I. Lasters: Fast and accurate side-chain topology and energy refinement (FASTER) as a new method for protein structure optimization. *Proteins* 48, 31–43 (2002)

**Footnotes:** [1] For those familiar with the formalism of the Dirac delta function, $g$ is the solution of the Poisson equation with the charge density, $\rho$ replaced by the three-dimensional Dirac delta function $\delta(\mathbf{r}-\mathbf{r}')$. [2] The above derivation is not valid in the case of the non-linear version of the Poisson–Boltzmann equation. Suitable energy expressions can be derived, but that is beyond the current scope of this article. [3] Sometimes the reference state is defined as having all ionizable group partial charges set to zero. In that case all four $W_{ij}$ may be non-zero. For example, if the neutral state is dipolar, one $W_{ij}$ is the charge–charge interactions, two are charge–dipole and one is dipole–dipole. Although it seems more complicated, such a scheme has some practical advantages in calculations including sidechain flexibility (47).

**Abbreviations:** MEAD: macroscopic electrostatics with atomic detail; LPB: linearized Poisson–Boltzmann; SOR: successive over-relaxation; PCM: polarized continuum model; SCRF: self-consistent reaction field; IMC: iterative mobile clustering.

**Key words:** Electrostatics, Protonation, Proton transfer, pKa, Review

**Send correspondence to:** Dr Donald Bashford, Dept. Molecular Biotechnology, Mail stop 312, Hartwell Center for Bioinformatics and Biotechnology, Saint Jude Children's Research Hospital, 322 N. Lauderdale St., Memphis, TN 38105-2794, Tel: 901-495-3970, Fax: 901-495-2945, E-mail: Don.Bashford@stjude.org